FUNDAMENTALS & APPLICATIONS

CHEMELECTROCHEM

ANALYSIS & CATALYSIS, BIO & NANO, ENERGY & MORE

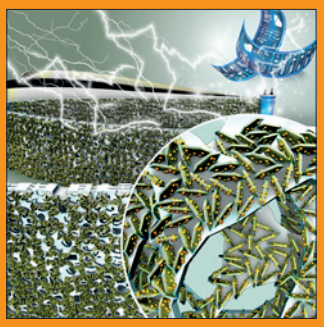
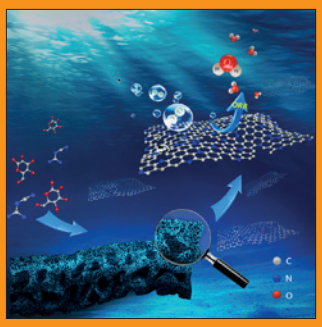
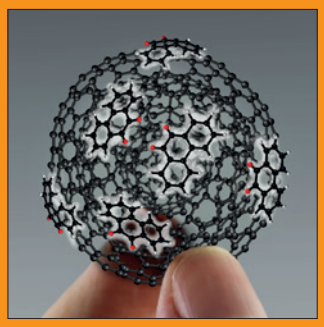
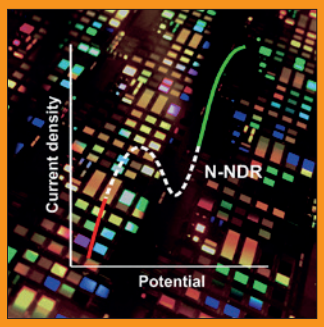

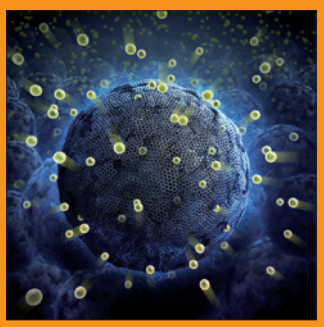



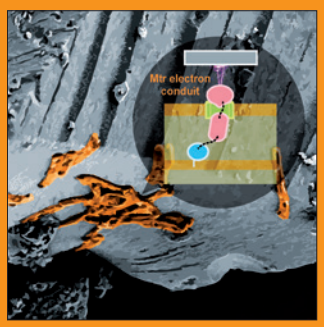

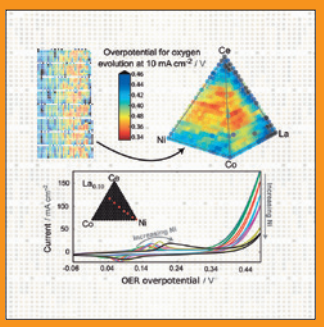

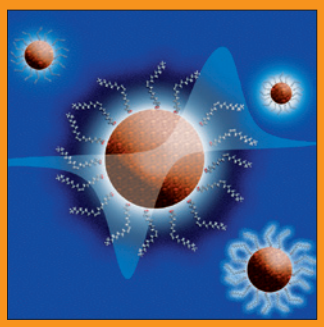
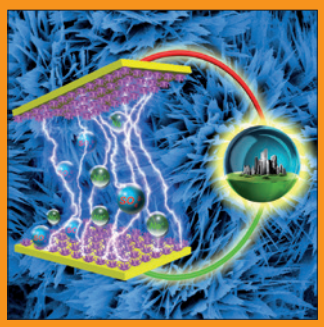
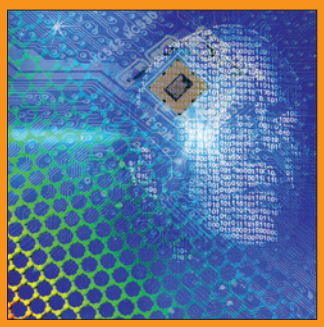

Reprint

A Journal of

WILEY-VCH

www.chemelectrochem.org

ChemPubSoc Europe

ChemPubSoc Europe

DOI: 10.1002/celc.201901435

CHEMELECTROCHEM Articles

Special Collection

Electrochemical Characterization of Nicotinamide Riboside

Sondrica Goines[a] and Jeffrey E. Dick*[a, b]

To improve quality of life, nicotinamide riboside (NR) has become a go-to supplement to serve as a precursor to nicotinamide adenine dinucleotide (NAD^+/NADH). NAD^+ is a cofactor used in various extra- and intra-cellular metabolic pathways by enzymes that maintain physiological functions like vision, hearing, and cognitive behavior. Unfortunately, innate NAD^+ levels decline over time giving rise to a need for NAD^+ boosters like NR to fight age-related diseases. To better understand redox pathways of NR in biological systems, we chose to study the electrochemistry of NR. Here, we electrochemically characterize NR in aqueous solutions using voltammetry, amperometry, bulk electrolysis, and mass spectrometry. We found the reduction of NR ($E_{p,c} = -1.1$ V vs. Ag/AgCl) is a diffusion-controlled reaction and calculated a diffusion coefficient of $4.6 \pm 0.1 \times 10^{-6}$ $cm^2 \cdot s^{-1}$. Square wave voltammetry indicated NR is reduced by one electron, and cyclic voltammetry suggested a major kinetic product, oxidizable at $E_{p,a} = +0.15$ V vs. Ag/AgCl. Bulk electrolysis confirmed the species at +0.15 V vs. Ag/AgCl was a kinetic product, and liquid chromatography-mass spectrometry of the bulk electrolysis products revealed the thermodynamic product was a dimer (NR_2). Finally, we studied the reduction of NR in whole cell lysate, which is shown to differ markedly from simple buffer solutions.

1. Introduction

We report the electrochemical characterization of nicotinamide riboside (NR), a popular precursor to nicotinamide adenine dinucleotide (NAD^+/NADH), which is a multifaceted, oxidoreductase cofactor within living cells.[1] NAD^+/NADH cofactor is critical for the success of the catalytic behavior of dehydrogenase enzymes, while also functioning as a biomarker within various systems and a regulatory agent for post-translational protein modifications.[2,3] In particular, NAD^+ determines the activity of enzymes, such as sirtuin enzymes, which are crucial to cellular metabolism, cell survival, and DNA repair.[4,5] The pyridine nucleotide is essential for the production and consumption of energy, and decreases in abundance as we age.[2,3,6] This has become apparent as the decline of the cofactor has been attributed to various disease states, such as cardiovascular disease, diabetes, and kidney failure.[7]

To highlight physiological relevance further, sirtuin enzymes use the cofactor to deacetylate the lysine groups of histones and proteins of various subcellular components.[5,8,9] Humans house seven orthologs of the enzyme with some found in the nuclei, cytoplasm, and mitochondria of mammalian cells.[5] Sirtuin enzymes improve metabolic efficiency by assisting in oxidative metabolism during times of exercise, calorie restriction, fasting, and low glucose.[9] They span proliferative and non-proliferative tissues linking them to the variety of disease states mentioned previously, as well as those that are neurodegenerative, when they are inactive. By 2050, $1 trillion will be spent yearly on those 65 years of age or older due to neurodegenerative diseases like dementia.[10] These findings justify the widespread interest of researchers in the study of NAD^+ levels in relation to sirtuin enzyme activity. Since NAD^+ is the rate limiting cofactor of sirtuin enzymes, the decline of the cofactor with age has been linked to steady declines in sirtuin activity. Furthermore, NAD^+ supplementation should promote healthy aging and an improved quality of life.[10–12] This suggests that with NAD^+ supplementation one may be able to sustain physiological functions that are known to decline with age such as vision, hearing, cognitive behavior, and motor functions.[13] A current and rather controversial question regarding the cofactor is whether one's healthspan or lifespan depends heavily on one's NAD^+ levels.

In an attempt to answer the question of whether the metabolite levels impact one's healthspan or lifespan, NAD^+ levels have been studied qualitatively and quantitatively using single cells, rodent models, and clinical trials.[7,8,14] Within the clinical trials performed by Martens and co-workers, physiological conditions are noted along with the concentration of the NAD^+ metabolome within blood mononuclear cells in correlation to chronic oral supplementation of NR.[7] The results of the chronic supplementation are also related to particular disease states typically found among middle-aged and older adults, such as heart disease, by noting particular physiological conditions like carotid artery compliance. The general consensus has been that vitamin B_3 supplementation improves one's healthspan, rather than one's lifespan.[7] Though many would like to combat ageing, one's lifespan may hang in the balance due to unavoidable damage to our biological systems, that may also be irreversible if one begins to look at age as a disease.[15]

The inevitable decline of NAD^+ is being combated through the use of oral supplements of the vitamin B_3 complex such as nicotinamide, nicotinic acid (niacin), nicotinamide mononucleo-

[a] S. Goines, Prof. J. E. Dick
Department of Chemistry
University of North Carolina at Chapel Hill
131 South Rd, Caudill Labs 340, Chapel Hill, NC 27599, USA
E-mail: jedick@email.unc.edu
[b] Prof. J. E. Dick
Lineberger Comprehensive Cancer Center
University of North Carolina at Chapel Hill
450 West Drive, Chapel Hill, NC 27514, USA

Special Collection An invited contribution to the Richard M. Crooks Festschrift.

tide (NMN), and NR, Figure 1, as well as sirtuin activating compounds like resveratrol.[2,6,8] As companies battle over rights to sell NR exclusively, scientists are exploring the inherent value of the supplement over the analogs previously listed.[16] Niacin was generally used as an NAD^+ booster until severe flushing and itching caused by the supplement deterred users. Additionally, there is no physiological evidence that niacin increases blood levels of NAD^+. NR has gained popularity as an alternative, and it has been shown to increase levels of NAD^+ in human blood during clinical trials.[11,13] NR, as well as NMN (i.e., the phosphorylated form), may be consumed daily from vegetables, fruits, and meat. NR and NMN may also be found in micromolar concentrations in milk produced by humans and cows.[11,17]

In an effort to begin understanding the redox pathways of NR, we present here an electrochemical characterization using a range of electrochemical techniques. Importantly, the workflow developed can be used as a foundation on which concentrations of unknowns can be elucidated. For instance, the biggest suppliers of NR are companies that sell a tablet. In principle, we show that one can purchase a tablet and attain the diffusion coefficient, number of electrons, and ultimately the concentration of the species of interest without the use of calibration curves, making the approach user friendly and amenable as a general strategy when approaching new molecules. The methods we chose to use allow one to begin to uncover the redox mechanism of the supplement in aqueous systems with minimal background information. This methodology may essentially be used to characterize a number of electroactive molecules that are biologically relevant with the caveat that the reactant and product for the heterogeneous reaction are freely-diffusing molecules. We show that the reduction of NR produces a thermodynamically stable dimerization product and that the fate of the kinetic product differs markedly in whole cell lysate than in buffer.

2. Results and Discussion

As a trending supplement, NR has become a compound of interest among researchers with the question of the compound's effect on healthspan or lifespan leading the discussion. Herein, the electrochemical characterization of NR offers a full view of the compound's redox characteristics without direct use of standards of known concentration. A typical cyclic voltammogram of NR is shown in Figure 2 on a characteristically inert glassy carbon macroelectrode ($r = 0.0015$ m). Electrochemical characterization of the supplement by the means outlined in this article may provide information concerning the mechanisms of NR dependent enzymes using the electrode/electrolyte solution interface as a model.[19]

2.1. Effect of Electrode Material

Initial experiments indicated that electrode material played a role in the mechanism of NR reduction. This is shown in Figure 3 as the peak potentials of NR reduction and product oxidation shift with respect to electrode material, indicating that the electrochemical reaction depends on the electrode surface and may have inner-sphere characteristics. Of note, the rate at which current rose during the reduction of NR varied greatly across different electrode materials, with glassy carbon (red curve) having the fastest rate. This finding is important since glassy carbon has a relatively wide potential window. The large current associated with Pt electrodes after NR reduction is assigned to proton reduction. Thus, future studies on the effects of NR within cells and tissues may use carbon-based materials, which are inert and allow for better electrochemical probing given their large potential windows under biologically relevant pH conditions compared to Au and Pt electrodes.

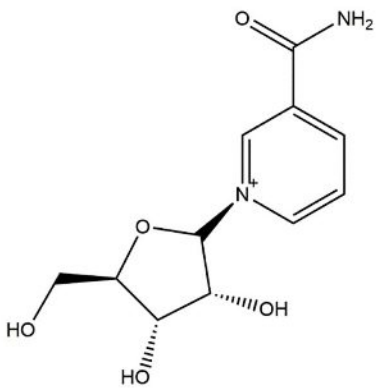

Figure 1. Chemical structure of nicotinamide riboside (NR, M.W. 255.25 g/mol).

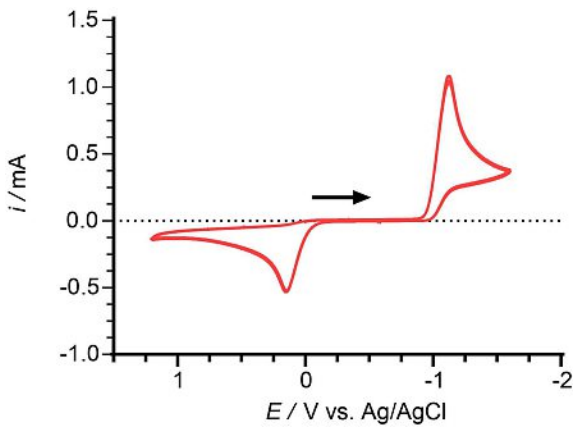

Figure 2. Cyclic voltammogram of NR capsule contents in 250 mM KCl on a glassy carbon (GC, $r = 0.0015$ m) macroelectrode versus a Ag/AgCl reference electrode, after sparging with N_2 gas, at a scan rate of 300 mV/s.

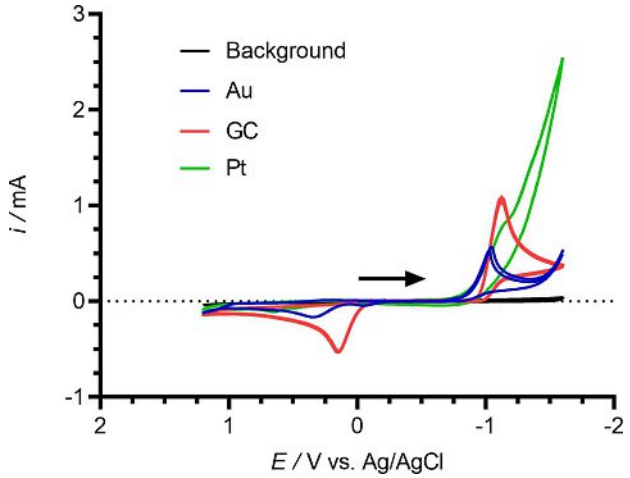

Figure 3. Cyclic voltammograms of NR capsule contents in 250 mM KCl on glassy carbon (GC, $r = 0.0015$ m), gold (Au, $r = 0.001$ m), and platinum (Pt, $r = 0.001$ m) macroelectrodes versus a Ag/AgCl reference electrode, after sparging with N_2 gas, at a scan rate of 300 mV/s.

2.2. Effect of pH

To gain an understanding of the effect of pH on the redox mechanisms of NR, 5 NR capsule samples of various pH values were prepared in 250 mM KCl. Cyclic voltammograms of each solution were obtained on a glassy carbon (GC, $r = 0.0015$ m) macroelectrode versus Ag/AgCl after sparging each solution with N_2 gas. The cyclic voltammograms in Figure 4 do not show variation in peak potential of NR reduction due to pH (generally ~59 mV per pH unit), indicating that the redox mechanism of NR reduction is not proton-coupled. Interestingly, however, the product of NR reduction, which has an oxidation potential around +0.15 V vs. Ag/AgCl, seems to depend on the pH environment, especially under acidic conditions. This will be the topic of future investigations, as supplement reactivity (and even cofactor reactivity) may change under low pH environments that are sustained during carcinogenesis with enhanced lactic acid generation (i.e., the Warburg Effect).

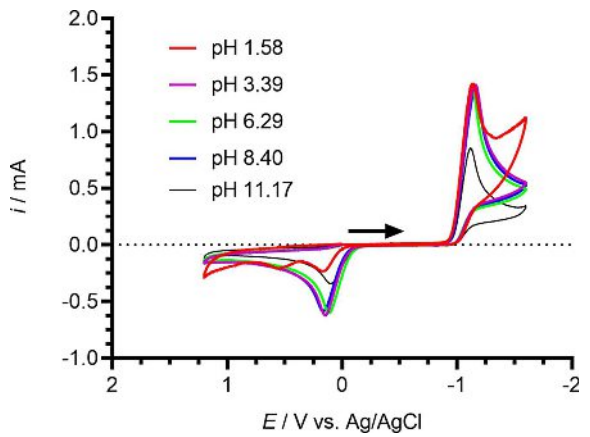

Figure 4. Cyclic voltammograms of NR capsule contents in 250 mM KCl at pH values ranging from 1.58 to 11.17 obtained at a GC ($r = 0.0015$ m) macroelectrode, after sparging with N_2 gas, at a scan rate of 500 mV/s.

2.3. Determination of the Diffusion Coefficient

In Figure 3, we showed the dependence of NR reduction on electrode material, indicating NR may adsorb onto the electrode material. Adsorption was further assessed by comparing the peak current versus scan rate (and square root of scan rate) at a glassy carbon macroelectrode. Cyclic voltammograms obtained to make this comparison are shown in Figure 5a.

The linear relationship derived between the square root of the scan rate and the average peak current in Figure 5c indicates that the redox mechanism follows the Randles-Sevcik equation, suggesting that the mechanism resembles a diffusion-controlled process instead of an adsorption process (i.e. the plot shown in Figure 5c is more linear than the plot shown in Figure 5b). In addition to data shown in Figure 3, discrepancies between the slope of each plot in Figures 5b & 5c are additional indications that weak adsorption does occur. It is important to note that these results indicate that there is a certain error associated with diffusion coefficient calculations discussed in this section.

Once it was determined that the rate of the redox reaction of NR is largely diffusion-controlled, chronoamperometry was employed to determine the diffusion coefficient. We chose this technique since the concentration of NR within capsule samples and number of electrons transferred during the reduction were still unknown. Chronoamperograms were taken at a gold ultramicroelectrode (Au UME, $r = 6.25$ μm) using a sample interval of 1 ms per point, termed the long-time region by Denuault and co-workers in 1991 when the method was developed.[18] At this region, the diffusion coefficient may be determined simply by Equation (1):

$$\frac{i_d(t)}{i_{d,ss}} = 1 + \left(\frac{2}{\pi^{\frac{3}{2}}}\right) a(Dt)^{-1/2} \quad (1)$$

where $\frac{i_d(t)}{i_{d,ss}}$ is the chronoamperometric current normalized by the steady state current, a is the radius of the electrode, D is the diffusion coefficient, and t is the time in seconds. Results are typically within 1% for t_i greater than one diffusion time frame.[18]

To approximate the diffusion coefficient, normalized current is plotted as a function of $t^{-1/2}$(Figure 6d). A linear regression of this plot was used to determine the slope and the intercept over the long-time region. The intercept in this region should be approximately 1 based on the literature.[18] The experimental diffusion coefficient was determined by Equation (2):

$$D = \frac{\pi a^2}{16S^2} \quad (2)$$

where a is the radius of the electrode and S is the slope of the linear regression.[18] The experimental data used to create the linear regression is presented in Figures 6b–c. As previously stated, this technique was done without prior knowledge of the number of electrons transferred (n) during NR reduction and the concentration of NR in solution. The average diffusion coefficient of NR was determined to be $4.6 \times 10^{-6} \pm 0.1$

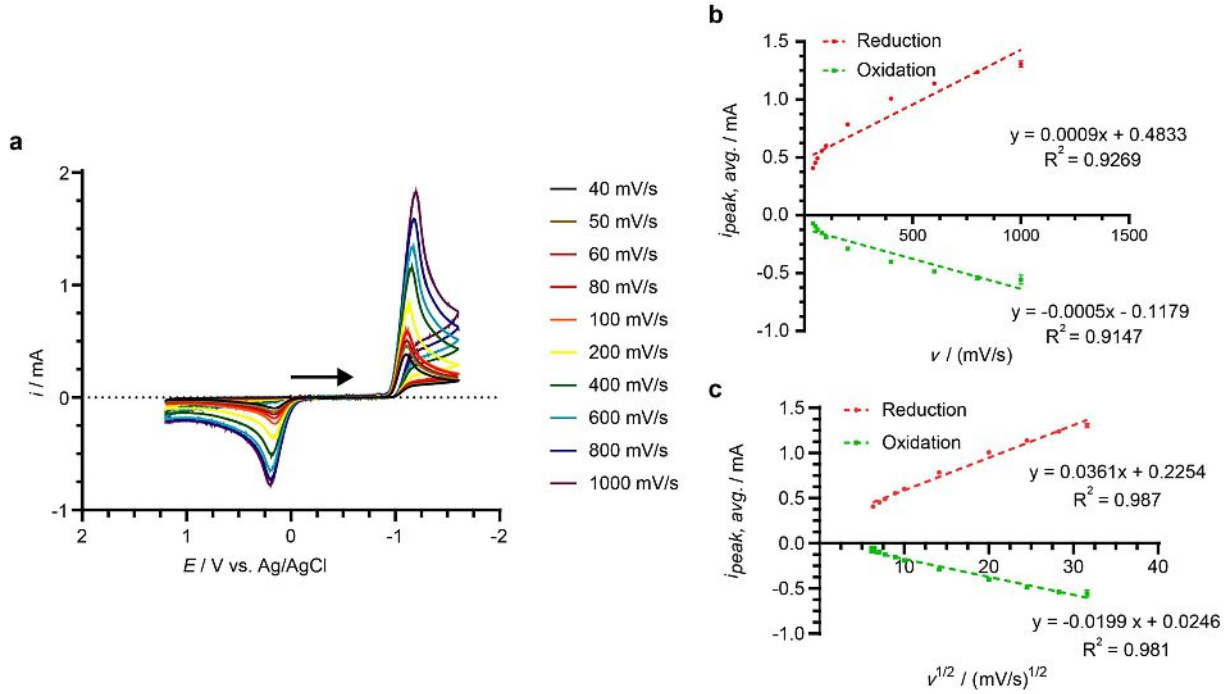

Figure 5. a) Cyclic voltammograms of NR capsule contents in 250 mM KCl, after sparging with N_2 gas, at scan rates ranging from 40 mV/s to 1000 mV/s obtained on a GC ($r = 0.0015$ m) macroelectrode versus Ag/AgCl. b) Linear regression trendlines for the average anodic and cathodic peak current versus the scan rate and c) the square root of the scan rate.

$\times 10^{-6}$ cm$^2 \cdot$s^{-1} ($N = 3$). This diffusion coefficient agrees qualitatively with that of NADH ($D = 2.4 \times 10^{-6}$ cm$^2 \cdot$s^{-1}) as the structure of NADH is larger than NR.[20]

2.4. Determination of the Number of Electrons Transferred (*n*)

In order to determine the concentration of NR by electrochemical means, the diffusion coefficient and number of electrons transferred (n) during the redox mechanism must be known. Square wave voltammetry, a pulse voltammetry technique valued for background suppression and sensitivity, was used to approximate the number of electrons transferred during NR reduction. In cases where the reactant and product are freely diffusing species, the full width at half of the maximum peak (FWHM) can be used as a diagnostic parameter for number of electrons transferred. A one-electron transfer event is represented by a FWHM of approximately 98 mV.[21] Oxidation of 1-hydroxymethylferrocene, a well-known one-electron transfer mediator, produced a FWHM of 97 ± 7 mV ($N = 6$), validating the use of the electrochemical technique (Figure 7 & inset). Reduction of NR is shown at more negative potentials ($E_{p,c} = -1.05$ V vs. Ag/AgCl) of the voltammogram in Figure 7 with an average FWHM of 101 ± 3 mV ($N = 5$), indicating a one-electron reduction mechanism. A Student's t-test at 95% confidence indicates that these FWHM values are statistically the same and that the null hypothesis cannot be rejected, providing further evidence that the number of electrons transferred during the reduction of NR is 1.

With the number of electrons transferred and the diffusion coefficient, the concentration of NR capsule contents soluble in 10 mL of 250 mM KCl was quantified by a cyclic voltammogram of the molecule on a GC macroelectrode ($r = 0.0015$ m) versus a Ag/AgCl reference. The average concentration determined using 6 TRU NIAGEN capsules was 47 ± 3 mM NR in 250 mM KCl. Both values were determined without the use of standards or a calibration curve.

2.5. Mechanistic Insight

Occasionally throughout the characterization process, two oxidation peaks were observed after the reduction of NR, with the oxidation peak between 0.13 V and 0.25 V vs. Ag/AgCl being consistently more dominant. These oxidation peaks were only observed after the reduction of NR, with the dominant peak assumed to be representative of the oxidation of the kinetic product. This characteristic is common amongst NAD^+ boosters and NAD^+. NAD^+ reduction is a one-electron transfer mechanism that results in the formation of a free radical species. Following the formation of the radical, the radical dimerizes. This dimer was described as the kinetically favorable product by Anne and co-workers in 1992.[22] Studies show that oxidation may result in two peaks due to oxidation of the radical species following cleavage of the dimer and oxidation of the dimer itself; one must note that the redox pathway of NAD^+ was hypothesized to follow an EC redox mechanism.[20,22]

Nicotinamide follows a similar reduction mechanism, but the reduction product may be oxidized by dissolved oxygen if

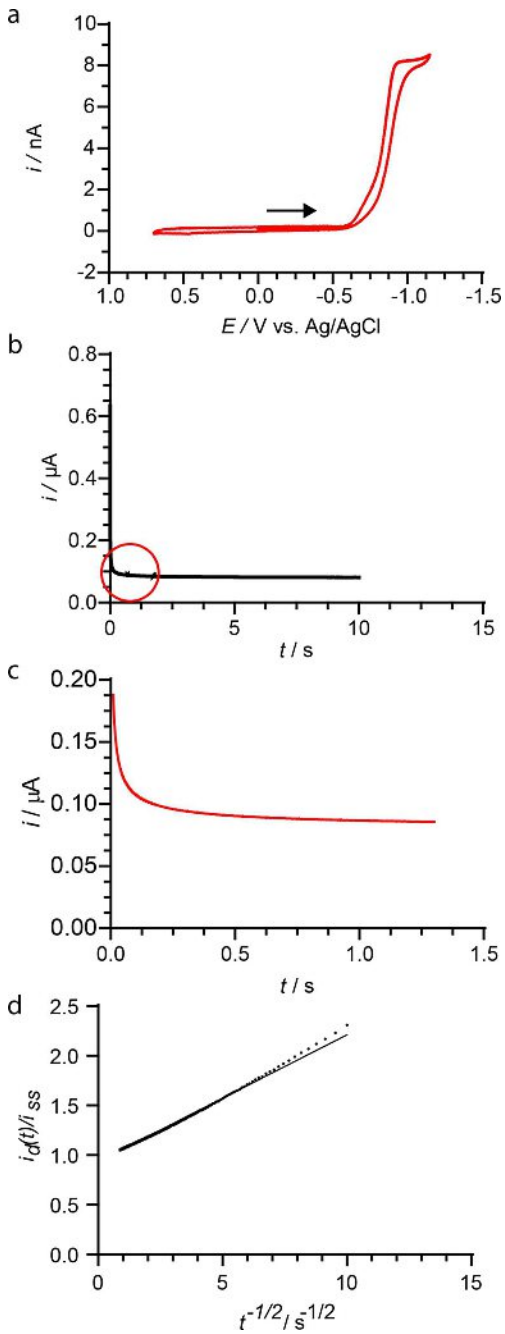

Figure 6. a) Cyclic voltammogram of NR capsule contents in 250 mM KCl at a Au UME ($r = 6.25$ µm) versus a Ag/AgCl reference electrode. b) Initial step of chronoamperogram of NR capsule contents in 250 mM KCl obtained, after sparging with N_2 gas, at the Au UME versus Ag/AgCl with the area of interest circled. c) The area of interest of a chronoamperogram of NR in 250 mM KCl. d) Linear regression of the normalized current versus the inverse square root of the time based on raw data shown in Figure 6c.

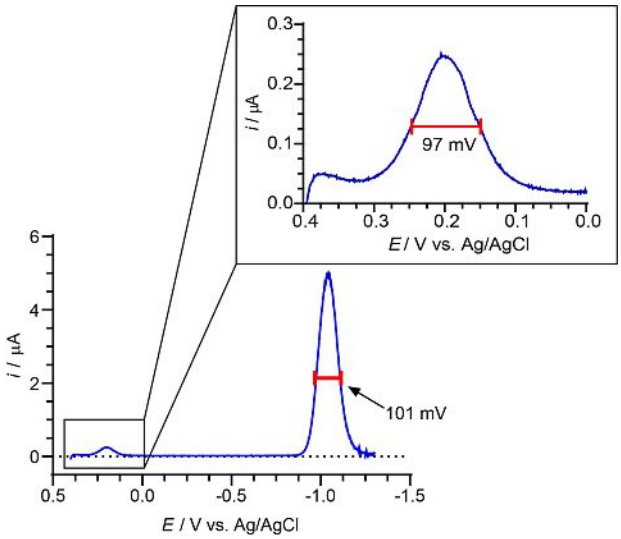

Figure 7. Square wave voltammograms of 1 mM ferrocene methanol (control) in 250 mM KCl and NR capsule contents in 250 mM KCl obtained on a GC macroelectrode ($r = 0.0015$ m) versus Ag/AgCl reference electrode. The red bar represents the FWHM.

substituted by an alkyl or hydroxyalkyl group on the nitrogen of the pyridine ring.[23] Furthermore, the chemical mechanisms of NR analogs suggest the formation of a kinetically favorable dimer following reduction of the analogs leading to the oxidation of the dimer and the radical species formed following cleavage of the dimer. Bulk electrolysis of NR (Figure 8b) was completed to investigate the mechanism with respect to NR and to determine the thermodynamic product of NR reduction (Figure 8a). Following bulk electrolysis, the final cyclic voltammogram showed two oxidation peaks of µA currents at approximately 0.25 V and 0.60 V vs. Ag/AgCl (Figure 8c) with the initial oxidation peak in Figure 8a being orders of magnitude larger. Though the final voltammogram showed the presence of two oxidation peaks at much lower currents, the voltammogram did not show currents near the magnitude of NR reduction pre-electrolysis. This indicates that some follow-up reaction occurs, and suggests the redox pathway follows the EC_{dim} mechanism (Schem 1). Importantly, our results indicate that the dimerized species, if formed, may not be the kinetic product. Furthermore, bulk electrolysis confirmed the square wave voltammetry results in that 1 electron is transferred during the reduction. Finally, the bulk electrolysis products were analyzed by liquid chromatography mass spectrometry (LCMS); in contrast to the redox mechanisms of NR analogs, LCMS data (Figure 9) displayed the dimer as the major product. Over two trials of bulk electrolysis, the major product peak was present at an m/z of 509.2 ± 2.3. Reduced or radical forms of NR were also observed in the background of the mass spectra of the product, but could not be differentiated due to limited resolution. Further confirmation of the thermodynamic product was evident in the absence of the dimer or reduced forms of NR within the standard sample. Additional LCMS data is contained in the Supplemental Information. From these results, we propose the oxidation peak at $+0.15$ V vs. Ag/AgCl is due to

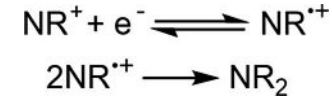

Scheme 1. EC_{dim} mechanism for the reduction of nicotinamide riboside.

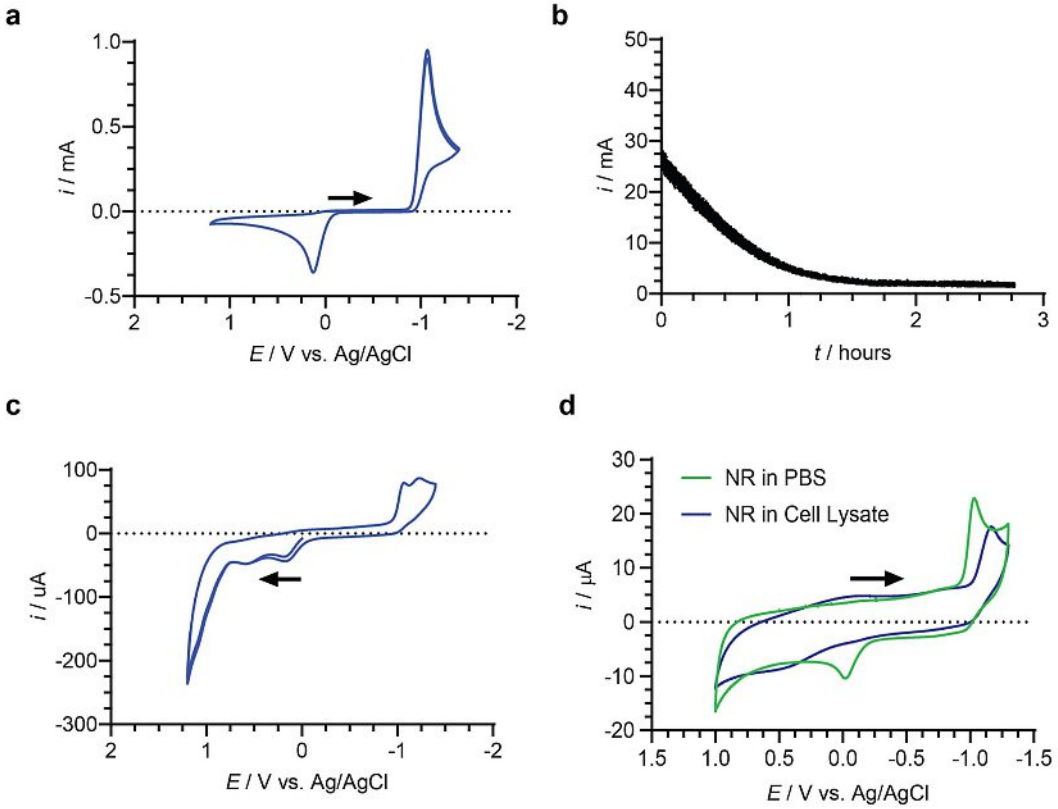

Figure 8. Bulk electrolysis experiment results showing: a) a cyclic voltammogram (CV) of NR in 250 mM KCl at a GC macroelectrode ($r = 0.0015$ m) versus a Ag/AgCl reference, b) an *i*–*t* trace of bulk electrolysis results at a GC rod verus Ag/AgCl, and c) a CV of the NR bulk electrolysis products in 250 mM KCl at a GC macroelectrode ($r = 0.0015$ m) versus a Ag/AgCl reference. A Pt coil wire was used as the counter electrode to collect Figures 8a–c. d) Cyclic voltammograms of 1 mM NR in Dulbecco's phosphate buffered saline and 1 mM NR in whole cell lysate of MRC5 P19 cells on a GC macroelectrode ($r = 0.0015$ m) versus a Ag/AgCl reference. A glassy carbon rod was used as the counter electrode.

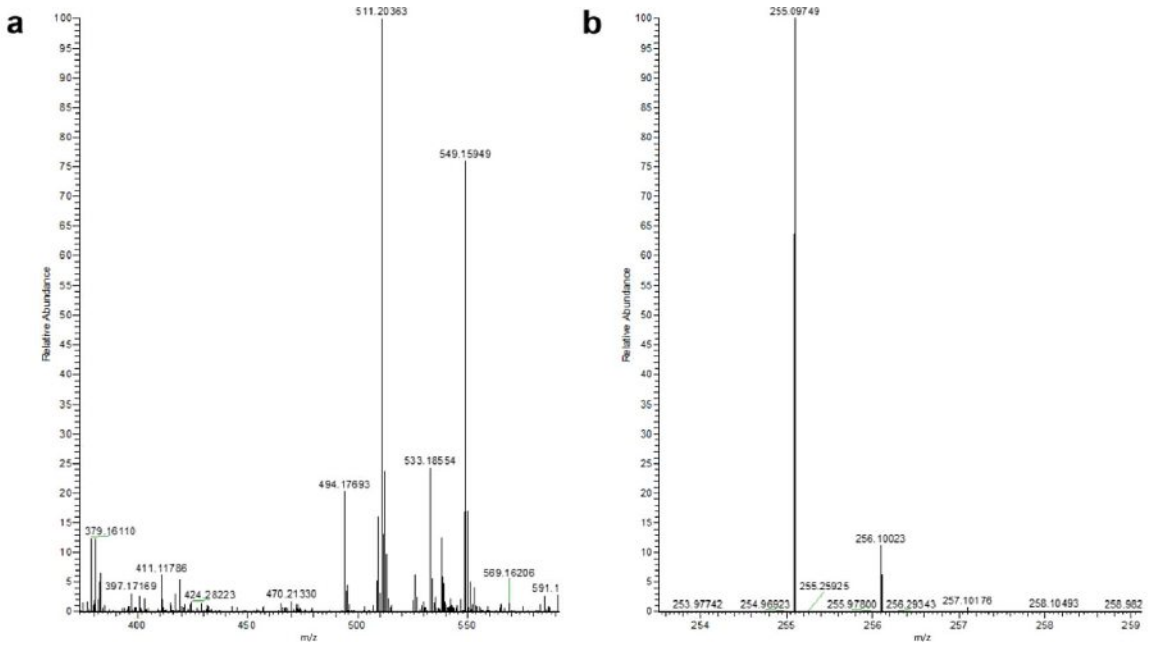

Figure 9. Mass spectra of the a) NR bulk electrolysis product and the b) NR standard.

the kinetic product, likely the radical before dimerization. The oxidation potential of the radical is much more positive than the reduction potential of NR, indicating a significant structural or solvation rearrangement after electron transfer.

The metabolism of NR to NAD^+ within the body is mediated by transferase and kinase enzymes. NR is phosphorylated by an NR kinase to produce NMN. Lastly, an adenylyl-transferase converts NMN to NAD^+.[17] Cyclic voltammograms of NR reduction in whole cell lysate depict a different redox pathway than the reduction of NR in buffer (Figure 8d). This observation may support the suggested active-site dependent model of NR metabolism in the body, indicative of inner-sphere behavior at the electrode surface.[24] While small shifts and kinetic effects may be due to non-specific adsorption of species on the electrode surface, the product peak differs most in whole cell lysate. Our new insight on the mechanism of NR reduction in aqueous systems provides the community with a better understanding of the potential pathways of NR prior to biosynthesis of NAD^+, while also providing electrochemical evidence of a pathway within human primary cells. Mechanistic insight into the reduction of NR in whole cell lysate will be a topic of future investigations.

3. Conclusions

Nicotinamide riboside (NR) is a biologically relevant compound with potential to improve quality of life during aging. The mechanism in which NR is involved in our metabolic pathways is a question of interest to better understand the use of NR supplements as NAD^+ boosters. The present study electrochemically characterized NR using a number of techniques based on the perspective that the electrode/electrolyte solution interface may be interpreted as a biological model. Based on the results of this study, the initial one-electron reduction of NR seemed to involve weak adsorption. The diffusion coefficient was determined without prior knowledge of the number of electrons transferred or the concentration of the analyte. Though the mechanism is slightly material dependent, NR reduction is not pH-dependent. We hypothesized reduction of the supplement is followed by a chemical reaction, in which the radical product of the reduction forms a more stable dimer (i.e., EC_{dim} redox mechanism). To determine the thermodynamic products of NR reduction„ bulk electrolysis was performed to generate the thermodynamic product. Bulk electrolysis was followed by cyclic voltammetry of the product and LCMS analysis. MS results confirmed the dimer as the major product. We conclude that NR reduction forms a radical species that dimerizes; however, this mechanism is shown to be different in whole-cell lysate.

Experimental Section

Reagents and Materials

Adenine (≥99%), D-(−)-Ribose (≥99%), β-Nicotinamide adenine dinucleotide sodium salt (NAD^+), Nicotinamide (≥99.5%), and potassium chloride were obtained from Sigma-Aldrich. Hydroxymethylferrocene (FcMeOH, 97%) was obtained from Alfa Aesar. Nicotinamide adenine dinucleotide (NADH), disodium salt (~100%, grade I) was obtained from Roche Diagnostics. Nicotinamide riboside in the form of TRU NIAGEN® supplement capsules were obtained from ChromaDex, Inc. All solutions were prepared using Milli-Q water (>18 MΩ·cm). Platinum foil was obtained from Fisher Scientific. Platinum wire coil was obtained from Pine Instruments (Durham, NC). Glassy carbon, platinum, and gold macroelectrodes were purchased from CH Instruments (Austin, TX) as well as platinum and gold ultramicroelectrodes (UMEs).

For cell maintenance, Dulbecco's Modified Eagle's Medium (DMEM) – high glucose and penicillin-streptomycin were purchased from Sigma-Aldrich. Dulbecco's phosphate buffered saline was purchased from Thermo Scientific. Premium grade 100% fetal bovine serum and 15.0 cm tissue culture dishes, sterilized and treated for increased cell attachment, were purchased from VWR International, LLC. Cells were kept in a Heracell™ VIOS 160i copper-lined incubator purchased from Thermo Scientific.

Instrumentation

Cyclic voltammograms were collected using CHI model 601E and 920D potentiostats (CH Instruments, Austin, TX). Platinum foil was typically used as the counter electrode, and the reference electrode was Ag/AgCl-sealed Pt wire (1 M NaCl). pH was measured using an AB 15 pH meter (Accument Basic, Fisher Scientific). Chronoamperograms were collected using the CHI model 601E, while square wave voltammograms were collected using the 920D model. Bulk electrolysis was performed with a WaveDriver 200 (Pine Instruments, Durham, NC).

Sample Preparation

For sample preparation, 250 mM KCl was prepared with Milli-Q water to be used as the standard electrolyte. A desired amount of a compound would be placed in 10 mL 250 mM KCl. If slightly insoluble, the sample was sonicated for approximately 15 minutes. Following sonication, the samples would be filtered using a 1 μm PTFE syringe filter. All samples were degassed with N_2 gas for 10 to 15 minutes prior to collecting data unless otherwise noted. N_2 gas was typically used as a blanket during data collection.

Effect of pH

Five NR capsule aqueous samples were prepared in 250 mM KCl. The pH of each solution was measured, then adjusted to five different pH values between 1 and 12 using a 1 M NaOH and a 20% v/v HCl solution. The HCl solution was prepared using a 37% HCl by weight stock solution. More basic solutions turned a deep yellow in comparison to the typical off-white color of NR samples. Cyclic voltammograms of each solution were obtained at a glassy carbon ($r = 0.0015$ m) macroelectrode versus Ag/AgCl at a scan rate of 500 mV/s. Pt foil was used as a counter electrode.

Effect of Electrode Material

Voltammograms of an NR capsule aqueous sample were captured at 300 mV/s at glassy carbon ($r = 0.0015$ m), platinum ($r = 0.001$ m), and gold ($r = 0.001$ m) macroelectrodes versus a Ag/AgCl reference electrode. Voltammograms were then overlaid for comparison.

Determination of Diffusion Coefficient

Voltammograms of an NR capsule aqueous sample were captured at scan rates between 40 mV/s and 1000 mV/s at a glassy carbon ($r = 0.0015$ m) macroelectrode versus a Ag/AgCl reference electrode. A linear regression was performed using an average peak current versus scan rate (ν) plot as well as an average peak current versus the square root of the scan rate ($\nu^{1/2}$) plot. These plots displayed evidence of a mass transfer-controlled reaction mechanism, giving us reason to determine the diffusion coefficient of NR *via* chronoamperometry. Chronoamperograms of an NR capsule aqueous sample were obtained using a gold UME ($r = 6.25$ μm). Data was collected between 0 and −1.3 V vs. Ag/AgCl at a sample interval of 1 ms (i.e. the long-time region).[18] A linear regression was performed on a normalized current vs $t^{-1/2}$ to determine the diffusion coefficient of the supplement.

Determination of Electrons Transferred

Square wave voltammograms of an NR capsule aqueous sample were obtained using a glassy carbon macroelectrode ($r = 0.0015$ m). The electrode was pulsed between 0 and −1.3 V vs. Ag/AgCl for data collection. Pt foil was used as a counter electrode.

Bulk Electrolysis of Nicotinamide Riboside & LCMS Analysis of the Product

An NR sample was prepared and filtered as done previously, and the 10 mL sample was placed in the middle component of a bulk electrolysis cell. On the left and right components of the cell, separated from the middle component by two frits, the counter and reference electrodes were submerged in 250 mM KCl, respectively. Prior to bulk electrolysis, a cyclic voltammogram was collected using a glassy carbon ($r = 0.0015$ m) macroelectrode vs. Ag/AgCl; a Pt wire coil was used as a counter electrode. The macroelectrode was replaced by a glassy carbon rod for bulk electrolysis. Bulk electrolysis of NR was performed at 1.2 V vs. Ag/AgCl for approximately 3 hours. During the experiment, the NR solution was bubbled with N_2 gas to increase mass transfer by convection to the glassy carbon rod. Following bulk electrolysis, an additional cyclic voltammogram was captured on a glassy carbon macroelectrode to characterize the product.

Following bulk electrolysis of NR, the product and an NR standard were analyzed with a Q Exactive HF–X (ThermoFisher, Bremen, Germany) mass spectrometer. Samples were introduced via a heated electrospray source (HESI) at a flow rate of 10 μL/min. One hundred time domain transients were averaged in the mass spectrum. HESI source conditions were set as: nebulizer temperature 100 deg C, sheath gas (nitrogen) 15 arb, auxillary gas (nitrogen) 5 arb, sweep gas (nitrogen) 0 arb, capillary temperature 250 degrees C, RF voltage 100 V. The mass range was set to 600–2000 m/z. All measurements were recorded at a resolution setting of 120,000. Solutions were analyzed at 0.1 mg/mL or less based on responsiveness to the ESI mechanism. Xcalibur (ThermoFisher, Breman, Germany) was used to analyze the data. Molecular formula assignments were determined with Molecular Formula Calculator (v 1.2.3). All observed species were singly charged, as verified by unit m/z separation between mass spectral peaks corresponding to the ^{12}C and $^{13}C^{12}C_{c-1}$ isotope for each elemental composition. Raw data is shown in the Supplemental Information.

Cyclic Voltammetry of Nicotinamide Riboside in Whole Cell Lysate

MRC5 cells P19, a human primary cell line, were maintained in a 15 cm tissue culture dish within a copper-lined incubator at 37 °C, 5% CO_2, and 10% O_2. Full growth media was composed of DMEM – high glucose, 10% fetal bovine serum, and 1% penicillin-streptomycin. At >75% confluence, spent media was removed from the tissue culture dish and cells were washed with 10 mL DPBS (1X). The tissue culture dish was charged with 45 mL of ultrapure H_2O, then placed on a shaker rotating at 30 rpm for approximately 1 hour and 30 minutes. Cell morphology was monitored every 10 minutes until cell lysis was confirmed. The lysate was centrifuged at 1000 rpm at 4 °C for 5 minutes. The supernatant was used to prepare 10 mL of 1 mM nicotinamide riboside chloride (M.W. 290.70 g/mol, 0.00316 g) in whole cell lysate. To fully dissolve nicotinamide riboside chloride, the solution was sonicated for 15 minutes. A background cyclic voltammogram of whole cell lysate was collected at a glassy carbon microelectrode ($r = 0.0015$ m) versus Ag/AgCl after purging the solution for 5 minutes. Using the same procedure, cyclic voltammograms of 1 mM nicotinamide riboside chloride in whole cell lysate and in DPBS (1X) were collected. A glassy carbon rod was used as the counter electrode to collect each cyclic voltammogram.

Acknowledgements

We acknowledge Daniel Conroy and Lettie A. Smith for their assistance with electrochemical analysis and Irene Dick for helpful discussion. We also acknowledge the University of North Carolina at Chapel Hill for start-up funds, which supported this work. We thank the University of North Carolina's Department of Chemistry Mass Spectrometry Core Laboratory, especially Brandie Ehrmann and Emily Wallace, for their assistance with mass spectrometry analysis. LCMS material is based upon work supported by the National Science Foundation under Grant No. (CHE-1726291).

Conflict of Interest

The authors declare no conflict of interest.

Keywords: electrochemistry · analytical methods · nicotinamide riboside

[1] S. Srivastava, *Clin. Trans. Med.* **2016**, *5*.
[2] M. V. Makarov, M. E. Migaud, *Beilstein J. Org. Chem.* **2019**, *15*, 401–430.
[3] A. Hikichi, H. Muguruma, H. Inoue, T. Ohsawa, *Electrochemistry* **2017**, *85*, 13–16.
[4] M. B. Schultz, Y. C. Lu, N. Braidy, D. A. Sinclair, *Adp-Ribosylation and Nad + Utilizing Enzymes: Methods and Protocols* **2018**, *1813*, 77–90.
[5] L. Mouchiroud, R. H. Houtkooper, J. Auwerx, *Crit. Rev. Biochem. Mol. Biol.* **2013**, *48*, 397–408.
[6] C. O. Schmakel, Santhana. Ks, P. J. Elving, *J. Electrochem. Soc.* **1974**, *121*, 345–353.
[7] C. R. Martens, B. A. Denman, M. R. Mazzo, M. L. Armstrong, N. Reisdorph, M. B. McQueen, M. Chonchol, D. R. Seals, *Nat. Commun.* **2018**, *9*.

[8] M. S. Bonkowski, D. A. Sinclair, *Nat. Rev. Mol. Cell Biol.* **2016**, *17*, 679–690.
[9] C. Canto, K. J. Menzies, J. Auwerx, *Cell Metab.* **2015**, *22*, 31–53.
[10] W. Giblin, M. E. Skinner, D. B. Lombard, *Trends Genet.* **2014**, *30*, 271–286.
[11] C. Canto, R. H. Houtkooper, E. Pirinen, D. Y. Youn, M. H. Oosterveer, Y. Cen, P. J. Fernandez-Marcos, H. Yamamoto, P. A. Andreux, P. Cettour-Rose, K. Gademann, C. Rinsch, K. Schoonjans, A. A. Sauve, J. Auwerx, *Cell Metab.* **2012**, *15*, 838–847.
[12] E. F. Fang, S. Lautrup, Y. J. Hou, T. G. Demarest, D. L. Croteau, M. P. Mattson, V. A. Bohr, *Trends Mol. Med.* **2017**, *23*, 899–916; H. C. Chang, L. Guarente, *Trends Endocrinol. Metab.* **2014**, *25*, 138–145.
[13] L. Rajman, K. Chwalek, D. A. Sinclair, *Cell Metab.* **2018**, *27*, 529–547.
[14] A. E. Kane, D. A. Sinclair, *Circ. Res.* **2018**, *123*, 868–885.
[15] J. A. Baur, Z. Ungvari, R. K. Minor, D. G. Le Couteur, R. de Cabo, *Nat. Rev. Drug Discovery* **2012**, *11*, 443–461.
[16] M. Bomgardner, *Chem. Eng. News* **2018**, *96*, 26–27.
[17] J. Yoshino, J. A. Baur, S. I. Imai, *Cell Metab.* **2018**, *27*, 513–528.
[18] G. Denuault, M. V. Mirkin, A. J. Bard, *J. Electroanal. Chem.* **1991**, *308*, 27–38.
[19] K. Takamura, A. Mori, F. Kusu, *Bioelectrochem. Bioenerg.* **1981**, *8*, 229–238.
[20] J. Moiroux, P. J. Elving, *J. Am. Chem. Soc.* **1980**, *102*, 6533–6538.
[21] A. J. Bard, L. R. Faulkner, *Electrochemical Methods: Fundamentals and Applications*, 2nd ed. (Eds.: D. Harris, E. Swain, C. Robey, E. Aiello), John Wiley & Sons, Inc., New York, NY, **2000**, pp. 261–304.
[22] A. Anne, P. Hapiot, J. Moiroux, J. M. Saveant, *J. Electroanal. Chem.* **1992**, *331*, 959–970; J. Moiroux, S. Deycard, T. Malinski, *J. Electroanal. Chem.* **1985**, *194*, 99–108.
[23] M. Miller, B. Czochralska, D. Shugar, *Bioelectrochem. Bioenerg.* **1982**, *9*, 287–298.
[24] J. A. Khan, S. Xiang, L. Tong, *Cell Press* **2007**, *15*, 1005–1013.

Manuscript received: August 30, 2019
Revised manuscript received: September 21, 2019